Scientia Iranica A (2021) 28(5), 2504–2518

Sharif University of Technology
Scientia Iranica
Transactions A: Civil Engineering
http://scientiairanica.sharif.edu

A semi-analytic method to estimate the response spectrum of the synthetic acceleration records with evolutionary spectrum

Z. Waezi[a,*] and M.A. Raoof[b]

a. *Department of Civil Engineering, Engineering School, Shahed University, Tehran, P.O. Box 33191-18651, Iran.*
b. *Department of Civil Engineering, Sharif University of Technology, Tehran, P.O. Box 11155-4313, Iran.*

Received 9 May 2020; received in revised form 29 November 2020; accepted 17 May 2021

KEYWORDS
Priestley's evolutionary process; First passage problem; Synthetic ground motion; Double-Frequency Model (DFM); power spectral density.

Abstract. In this paper, we introduce a semi-analytic procedure for deriving the response spectrum of the synthetic acceleration records generated using the Double-Frequency Model (DFM). DFM is a filtered white noise method for fully non-stationarity synthetic acceleration records. The proposed semi-analytic procedure is based on the theory of the first passage problem, which precludes time and computationally extensive methods such as Monte Carlo simulations. Assuming a slowly-varying envelope and evolutionary transfer functions, the procedure of estimating the elastic response of a structure is implemented in both time and frequency domains. Comparing the results of our model with previous models and approximations, we concluded that for a set of 10000 realizations of the DFM model, the semi-analytic model produces an error of less than 10% for 92% of the realizations. The accuracy of estimations is higher in the short-period compared to the long-period ranges of the response spectrum. Comparing the accuracy of approximations used to arrive at peak factors, results show that Michaelov approximation executed in the frequency domain yields the best results compared to Poisson or Vanmarcke procedures.

1. Introduction

In recent years the tendency toward the development of synthetic ground motions has grown extensively. There are generally physical, stochastic, and hybrid models to generate artificial earthquake motion. The popularity of stochastic methods which aim to regenerate the statistical characteristics of the recorded motions has soared in recent years. Stochastic ground-motion models are generally of two types: 'source-based' and 'site-based' [1]. Although the source-based models have the advantage of using the physical parameters obtained through simulation processes, with due attention to the seismological nature of the region, these parameters vary significantly from region to region. On the other hand, since site-based models do not require detailed seismological information, they are more advantageous when the number of instrumental recordings is limited [2]. Due to the capability of the stochastic methods in generating high-frequency signals [3,4] and the availability of fast computers, pure "physical models" have evolved to the "hybrid models" using stochastic methods and thus formed powerful tools to simulate ground motions for scenario-based earthquake simulation.

Depending on the time variation of its amplitude

*. *Corresponding author. Tel.: +98 21 51212108*
E-mail addresses: waezi@shahed.ac.ir (Z. Waezi); m.amin.raoof@gmail.com (M.A. Raoof)

doi: 10.24200/sci.2021.55925.4474

and frequency content, an earthquake accelerogram as a signal can be categorized either as stationary or non-stationary. The amplitude non-stationarity is defined as the change in the amplitude or intensity of the acceleration record versus time, while the frequency non-stationarity indicates the change of its "instantaneous power spectrum" [1]. The frequency non-stationarity of the signal originates from the dynamic characteristics of ground motion, which is mainly due to the fast propagation speed of high-frequency waves in the soil medium [5]. Many studies indicate the significance of the frequency content change on the seismic-induced response of linear and nonlinear structures [6]. The simultaneous occurrence of the decrease in stiffness and the arrival of low-frequency surface waves could lead to catastrophic results and even the collapse of these structures [7].

Contrary to the amplitude non-stationarity, it is hard to simulate or even capture the frequency non-stationarity of the signals. Some methods have been introduced to consider the non-stationarity of the recording, especially in the frequency domain, some of which involve a large number of parameters [2,8–12]. Accurate detection of the frequency content evolution demands the utilization of complex time-frequency distributions (such as quadratic distributions) or multi-resolution analyses (such as wavelet or Hilbert-Huang transforms). On the other hand, the proper representation of these variations requires a considerable amount of data. Two main methods have been used in recent studies to generate fully nonstationary earthquake records: 1) filtered white-noise models and 2) spectral representation models. The filtered white noise model is generally described as a convolution integral of an input white noise and an evolutionary Impulse Response Function (IFR) [13]. The spectral representation is generally stated as the sum of the modulation of the different harmonics with a random phase but extended versions of the model are also proposed [14].

After the development of the models proposed by Rezaeian and Der Kiureghian [1,15] multiple studies have been published with a similar approach that incorporated the ground motion variability in their models through paying special attention to the correlation of the model parameters with the earthquake scenario parameters.

Waezi and Rofooei [16,17] introduced a new site-based method for the stochastic generation of non-stationary acceleration records. The proposed model is capable of considering two large and one small dominant frequency for efficient capturing of recorded strong motion's power spectrum. They also proposed a High-Pass-Filtered (HPF), time-varying, Double-Frequencies Model (DFM) with time-variant parameters to simulate a frequency-wise non-stationary process. Moreover, they included a method for scenario-specific record simulation using DFM [18].

Having the synthetic record, it is desirable to estimate the distribution of the response of the structures subjected to these excitations given that their model parameters are fixed. This can help develop methods to generate acceleration records whose response spectrum is compatible with those specified in the seismic design code [19]. This is important because common methods of generating spectrum compatible records usually use seeds to accelerate the time history and change its frequency content through trial and error schemes to achieve the best compliance. However, this method ignores the correlation between different harmonics in the time history of ground motions, and only captures the compliance of the response spectrum.

One of the methods to determine the response of the structures to non-stationary excitation is through the 'first passage problem' which could be referred to as Extreme Value Distribution (EVD) theory or peak-factor problem. In recent decades, due to the increasing interest in performance-based design, the acquisition of peak factor in earthquake engineering has received a great deal of attention [20]. Derivation of analytical equations for structures is straightforward when the response of the structure is stationary, but assuming the oscillator response to be non-stationary, calculating the peak response turns to an extensive process since several convolution multiplications should be conducted to determine the spectral specifications of the structure response process, and also a nonlinear integral equation should be solved to evaluate the peak response [21].

Since the peak response is a random variable, it can be comprehensively described by its Cumulative Distribution Function (CDF) or probabilistic distribution function. Although it is common to use average values of peak responses for design purposes, this is not a conservative approach because structural responses could exceed them. Nevertheless, using a direct method, in which the design level is determined by a response level of a certain non-exceedance probability, seems to be more rational; this level is called the "quantile (percentile) level". It can be proved that calculating the quantile level is easier than calculating the mean and the standard deviation of peak response [22]. The major problem in estimating the 3 parameters of the value of the mean, standard deviation, and the quantile level of response, is that the mathematical form of the peak CDF of the structural response is unknown. Traditionally, this task has been addressed thanks to the computation power of modern computers and numerical methods; however, the complexity of these problems and the amount of time needed to obtain the exact result is a disadvantage that could prevent designers from using such methods [22].

A large number of studies have been conducted on the reliability evaluation of structures under non-stationary excitations, but most of the studies have focused on the excitations generated using spectral representation methods. Barbato and Vasta [23] developed a method for estimation of the evolutionary parameters of the non-classically damped Multi Degrees-Of-Freedom (MDOF) linear systems subjected to the time-modulated colored noise excitation. Barbato and Conte [24] extended the concept of bandwidth factor to complex-valued non-stationary processes, from which they evaluated the reliability of non-classical damped MDOF structures under Kanai-Tajimi [25] amplitude non-stationary excitations. Barbato and Conte [26] developed a method to find the reliability of the non-classically-damped MDOF which is subjected to a completely non-stationary random excitation described by a spectral representation. Alderucci and Muscolino [27] proposed a method to generate a specific type of fully non-stationary synthetic records compatible with a design code based on the solution of the 'first passage problem'. Yu et al. [28] derived an approximate solution of the time-domain random response of a linear MDFO system under completely non-stationary excitation described using the spectral representation method. To reduce the computation cost of the evaluation of the stochastic response of MDOF large-scale structures based on random vibrations theory, Zhao and Huang [29] proposed an approach involving Fast Fourier Transform (FFT). They also used a spectral representation to describe the nonstationary random excitation. Alderucci et al. [27] analyzed and evaluated the time-frequency response function of a non-classical damped MDOF structure under the relevant completely non-stationary excitation. Xu and Feng [30] proposed a new high-order variable space point selection method, which uses the probability density evolution method of completely non-stationary ground motion represented by the spectral representation to obtain the reliability of the nonlinear system numerically. Xu et al. [31] used nuclear density distribution and Latin hypercube simulations and found that the nonlinear structure fails with a small probability under the action of non-stationary ground motion expressed in spectral representation.

In this paper, the approximate maximum oscillation response of the structures, subjected to a non-stationary excitation generated by the DFM model, a filtered white noise model, is studied. The purpose of this paper is to determine a semi-analytic relationship to describe the response of a linear elastic structure to non-stationary excitations simulated by DFM. At first, the modulating function and the evolutionary power spectrum are expressed in terms of the model parameters using some simplifications.

Then the maximum peak factor is calculated by a semi-analytical method, which eliminates the need for a large number of calculation simulations, and evaluates the efficiency of the proposed method.

2. Double-Frequency Model (DFM) model

The DFM, is a site-based filtered white noise stochastic method proposed by Waezi et al. [16,18,32], which is capable of generating both amplitude and frequency non-stationary records, with 13 model parameters. It was shown that the 13 model parameters can be regressed against source-path-site characteristics which enable the model to generate an ensemble of records conditioned on a specific scenario. The DFM method, which can incorporate both the amplitude and frequency non-stationarity, can be stated as:

$$a\left(t\right)=q\left(t\right)\left\{\frac{1}{\sigma\left(t\right)}\int_{-\infty}^{t}h\left(t-\tau,\tau\right)w\left(\tau\right)d\tau\right\}, \qquad (1)$$

where $a(t)$, $q(t)$, $h(t,\tau)$, and $\sigma(t)$ represent the synthetic acceleration record, Envelope Function (EF), evolutionary IRF of the model, and standard deviation of the process resulted from the integral in Eq. (1), respectively. Considering that $w\ (\tau)$ is a stationary white noise with constant Power Spectral Density (PSD) equal to S_0, the evolutionary variance of the resulted non-stationary process $a(t)$ can be described as:

$$\sigma^2\left(t\right)=2\pi S_0\int_0^t h(t,\tau)^2 d\tau. \qquad (2)$$

The evolutionary IRF of DFM is defined according to the inverse Fourier transform of a complex function called the Evolutionary Transfer Function (ETF). ETF of DFM is outlined as follows:

$$H\left(\omega,t\right)=\frac{1-\frac{2i\xi_f(t)\omega}{\omega_f(t)}}{1-\frac{\omega^2}{\omega_f(t)^2}-\frac{2i\xi_f(t)\omega}{\omega_f(t)}}\times\frac{1-\frac{2i\xi_g\omega}{\omega_g}}{1-\frac{\omega^2}{\omega_g^2}-\frac{2i\xi_g\omega}{\omega_g}}, \qquad (3)$$

where $\xi_f(t)$ and $\omega_f(t)$ represent the damping and the frequency parameter of the time-variant part of the ETF while ξ_g and ω_g denote their counterpart for the stationary part of ETF. This model is capable of encompassing two distinct PSD peaks, which is not uncommon in the recorded ground motions. The DFM is an adjustment to the Modified Kanaii-Tajimi (MKT) model, used to capture the PSD low-frequency region of the obtained synthetic records. It is assumed here that $\xi_f(t)$ and $f_f\left(t\right)=\frac{\omega_f(t)}{2\pi}$ are linear functions of time as:

$$f_f\left(t\right)=f_{f_0}+\frac{f_{f_n}-f_{f_0}}{T_d}t,$$

$$\xi_f\left(\mathrm{t}\right)=\xi_{f_0}+\frac{\xi_{f_n}-\xi_{f_0}}{T_d}t, \qquad (4)$$

where T_d represents the effective duration of the records

and "0" and "n" subscripts indicate the value of the time-variant parameters (i.e. ξ_f and f_f) at the beginning and the end of the effective duration of the acceleration time-history. For the sake of simulation, the effective length of the record is adopted as the duration between the times corresponding to 0.1% and 99.9% of the maximum Arias intensity.

The EF $q(t)$ in Eq. (1) is used to curb the evolutionary variance of the simulated process independently from the frequency content. Because of its higher flexibility, Amin and Ang [33] envelope function is used as EF in this paper:

$$q(t)=\begin{cases}0 & t\le T_0\\ \alpha_1\left(\frac{t-T_0}{T_1-T_0}\right)^2 & T_0\le t<T_1\\ \alpha_1 & T_1\le t<T_2\\ \alpha_1\exp\left[-\alpha_2(t-T_2)\right]^{\alpha_3} & t\ge T_2\end{cases} \tag{5}$$

The EF parameters, listed as $\alpha = \{T_0, T_1, T_2, a_1, a_2, a_3\}$, are determined according to the best fit of Arias intensity of Amin and Ang's modulating function to the target Arias intensity curve of the record. The authors have determined the range of variation of EF parameters according to the values obtained for non-pulse-like near-field ground motions for the previous study [18,32]. It should be mentioned that since T_0 only shifts the modulating function in time, it can be set equal to zero, and consequently T_1 and T_2 are shifted as $T_1^* = T_1 - T_0$ and $T_2^* = T_2 - T_0$.

To make the velocity time-histories obtained from the DFM model approach zero at the end of the time series, the components having near-zero frequencies should be carefully filtered out without disrupting the low-frequency components. For this purpose, the relative acceleration response of an Single Degrees-Of-Freedom (SDOF) $\ddot{u}(t)$, which is subjected to the generated DFM acceleration record $a(t)$ is used. This response, hereinafter referred to as a HPF can be expressed as follows:

$$\ddot{u}+2\xi_c\omega_c\dot{u}+\omega_c^2 u=-a(t), \tag{6}$$

where u, $\ddot{u}$, and $a(t)$ denote the SDOF's relative displacement, acceleration, and excitation process derived from Eq. (6), respectively, and ξ_c and $\omega_c = 2\pi f_c$ represent the damping and frequency of the HPF. $\ddot{u}$ is hereafter used as the record simulated using DFM and will be referred to as $a_{DFM}(t)$. Therefore, the Evolutionary Power Spectral Density (EPSD) of DFM records depends on 13 parameters including 8 IRF parameters $\left\{\xi_g, f_g, \xi_{f_{mid}}, \xi_f^{'}, f_{f_{mid}}, f_f^{'}, \xi_c, f_c\right\}$ and 5 EF parameters (assuming $T_0 = 0$) $\{T_1^*, T_2^*, a_1, a_2, a_3\}$.

3. DFM's evolutionary power spectrum

According to Priestley [34], a real-valued stochastic evolutionary process can be defined as the general form of Fourier-Stieltejes as follows:

$$X(t)=\int_{-\infty}^{+\infty} A(t,\omega)\exp(i\omega t)\,dZ(\omega), \tag{7}$$

where $A(t,\omega)$ is a deterministic complex-valued modulating function and $Z(\omega)$ is a random complex-valued function. $X_s(t)$ is the "embedded" stationary process which is defined based on its spectrum as follows:

$$X_s(t)=\int_{-\infty}^{+\infty}\exp(i\omega t)\,dZ(\omega), \tag{8}$$

in which:

$$E[dZ(\omega_1)\,dZ(\omega_2)]=S_{XX}(\omega_1)\,\delta(\omega_1+\omega_2)\,d\omega_1 d\omega_2, \tag{9}$$

where $S_{XX}(\omega)$ is representative of the PSD of the stationary process $X_S(t)$ and $\delta(.)$ is Dirac delta. If the Fourier Transform of $A(t,\omega)\exp(i\omega t)$ on ω axis is available, Eq. (7) can be stated in the time domain using a convolution integral as:

$$\psi(t,\tau)=\frac{1}{2\pi}\int_{-\infty}^{+\infty} A(t,\omega)\exp[i\omega(t-\tau)]\,d\omega,$$

$$A(t,\omega)\exp(i\omega t)=\int_{-\infty}^{+\infty}\psi(t,\tau)\exp[i\omega\tau]\,d\tau. \tag{10}$$

Then final expression for $X(t)$ is:

$$X(t)=\int_{-\infty}^{+\infty}\psi(t,\tau)\,X_S(\tau)\,d\tau. \tag{11}$$

For $X(t)$, EPSD is stated as follows:

$$G_{XX}(t,\omega)=|A(t,\omega)|^2 S_{XX}(\omega). \tag{12}$$

Differentiating Eq. (7) for j times gives:

$$X^{(j)}(t)=\int_{-\infty}^{+\infty} A_{(j)}(t,\omega)\exp(i\omega t)\,dZ(\omega), \tag{13}$$

where $X^{(j)}$ is the jth derivative of $X(t)$ and $A_{(j)}$ is the modulating function for $X_{(j)}(t)$ that can be obtained using the following recursive formula:

$$A_{(j)}(t,\omega)=\dot{A}_{(j-1)}(t,\omega)+(i\omega)\,A_{(j-1)}(t,\omega). \tag{14}$$

Comparing Eq. (11) with Eq. (1), one can express $\psi(t,\tau)$ corresponding to DFM as:

$$\psi(t,\tau)=\alpha(t)\,U(\tau)\,h(t-\tau,\tau), \tag{15}$$

where $U(\tau)$ is the unit step function to count for the lower bound of the integral used in Eq. (1) and substituting Eq. (15) in Eq. (10) gives:

$$A(t,\omega)=\alpha(t)\int_{-\infty}^{+\infty} U(\tau)\,h(t-\tau,\tau)\,\exp[-i\omega(t-\tau)]\,d\tau, \tag{16}$$

and by a change of integration variable τ to s it gives:

$$A(t,\omega)=\alpha(t)\int_0^t h(s,t-s)\exp[-i\omega s]\,ds. \tag{17}$$

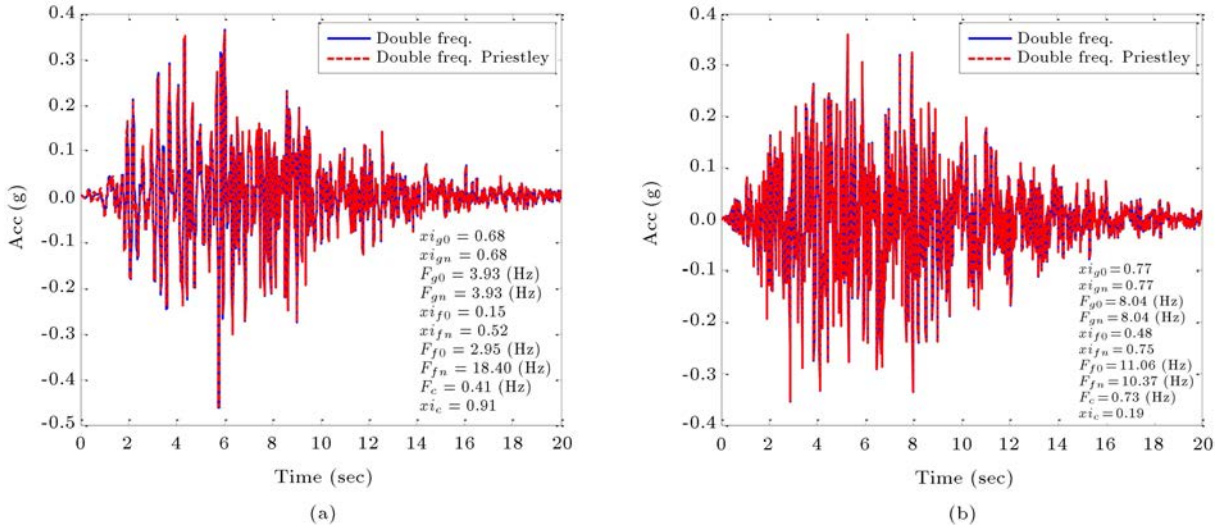

Figure 1. Comparison of time history records of double-frequency model in two cases of (a) Priestley's formulation and (b) DFM's formulation.

Furthermore, $h(t-\tau,\tau)$ in DFM is calculated from ETF, $H(\tau,\omega)$, as follows:

$$h(s,\tau) = \int_{-\infty}^{+\infty} H(\tau,\omega)\exp(i\omega s)\,d\omega,$$

$$H(\tau,\omega) = \frac{1}{2\pi}\int_{-\infty}^{+\infty} h(s,\tau)\exp(-i\omega s)\,ds. \tag{18}$$

Comparing Eq. (18) with Eq. (8), the large differences between $H(\tau,\omega)$ and $A(t,\omega)$ becomes evident:

$$h(s,t-s) = \int_{-\infty}^{+\infty} H(t-s,\sigma)\exp(i\sigma s)\,d\sigma,$$

$$A(t,\omega) = \alpha(t)\int_{-\infty}^{+\infty}\exp[-it(\omega-\sigma)]\int_0^t H(\tau,\sigma)$$
$$\exp[i(\omega-\sigma)\tau]\,d\tau d\sigma. \tag{19}$$

Having obtained the complex modulating function of the DFM records, their EPSD can be calculated applying Eq. (12). However, another model can be proposed with a given $H(t,\omega)$ in a way that in this model $H(t,\omega) = A(t,\omega)$ and it gives:

$$\psi(t,\tau) = \frac{1}{2\pi}\int_{-\infty}^{+\infty} H(t,\omega)\exp[i\omega(t-\tau)]\,d\omega,$$

$$h(t-\tau,t) = \int_{-\infty}^{+\infty} H(t,\omega)\exp[i\omega(t-\tau)]\,d\omega. \tag{20}$$

In such a case, we have:

$$\psi(t,\tau) = \alpha(t)\,U(\tau)\,h(t-\tau,t). \tag{21}$$

It should be noted that the second variable of h in Eq. (21) is different from that of Eq. (15). The difference springs from $h(t-\tau,t)$ which indicates that the response of an impulse exerted at τ and recorded at t is dependent on the parameters at t. However, in the DFM case, if impulse exerted at τ and recorded at t the response is dependent on τ. It can be proved that, if $H(\tau,\omega)$ has a slow variation versus time:

$$h(t-\tau,\tau) \cong h(t-\tau,t),$$

$$A(t,\omega) \cong H(t,\omega). \tag{22}$$

Figure 1 shows a record generated using $h(t-\tau,t)$ in Eq. (1) for DFM, which is called Priestly Double-Frequency Model, with those of original DFM with $h(t-\tau,\tau)$ in Eq. (1) which is denoted as double-frequency. The results show that only when the variation rate of model parameters is high, the differences are noticeable.

4. Peak value problem

Let's assume that $X(t)$ is the displacement response of an elastic SDOF with natural frequency ω_0 and damping ratio ξ_0 subjected to a random excitation generated by the DFM. One technique for formulating the peak response of an SDOF is to define a new random process $\{Y(t)\}$, which is the peak value of $\{X(t)\}$ up to t. In other words:

$$Y(t) = \max_{0\le s\le t} X(s). \tag{23}$$

Peak value distribution for $X(t)$ is similar to the distribution of the random parameter $Y(t)$. For a stationary random process $\{X(t)\}$, it should be expected for $\{Y(t)\}$ to be non-stationary, since, if the study time is extended, higher values of $X(t)$ will be noticed. If $L_X(u,t)$ is considered as the CDF of $Y(t)$:

$$L_X(u,t) = F_{Y(t)}(u) \equiv P[Y(t)\le u]$$
$$\equiv P[X(s)\le u : 0\le s\le t]. \tag{24}$$

The last term indicates that $X(s)$ is less than or equal to u for all values of s. $L_X(u,t)$ is sometimes called the survival probability. Often, expressing the survival probability as a form of the time-exponential function is convenient. In certain conditions one can write:

$$L_X(u,t) = L_X(u,0)\exp\left(-\int_0^t \eta_X(u,s)\,ds\right), \quad (25)$$

where $\eta_X(u,t)$ is regarded as the conditional rate of up-crossing from level u, given that no earlier up-crossing has occurred. If the up-crossing from level u is taken as the failure in a system, $\eta_X(u,t)$ is called the risk function in the reliability field.

There is no exact analytical relationship for $\eta_X(u,t)$, however, some simplifying assumptions are made to determine it. In this study, three assumptions are used to evaluate the response spectrum of the DFM records. These methods are summarized in the following subsections.

4.1. Poisson's assumption

The simplest method is to assume that b level crossing occurs independently in time t. For an upper bound level of b, we could assume that the crossing occurrences to be independent, especially for broad-band processes, and it seems that this assumption is acceptable [22,35]. The Poisson approximation of $\eta_X(u,t)$ is shown as $\eta_X^P(u,t)$, which is represented for a symmetrical and two-sided barrier process of b and can be expressed as follows:

$${\eta_X}^P(b,t) = 2\nu^+(b,t), \quad (26)$$

where $\nu^+(b,t)$ is equal to the expected exceedance rate in b level by $X(t)$ at any time t. It can be proved that this approximation for a short time interval of t or a narrow-band process is too conservative. It is shown that the exceedances of narrow-band processes usually tend to cumulate in a cluster-like form, and this fact contradicts the independency assumption [22]. Shinozuka and Yang proposed an approximation to calculate the mean and standard deviation of the peak responses of random processes in wide time intervals [36]. Since, in this paper, short-length records are studied, these equations are not acceptable. To evaluate $\nu^+(b,t)$, the following classic result can be used:

$$\nu^+(b,t) = \left[\frac{\sigma_{\dot{X}}\left(1-\rho_{X\dot{X}}^2\right)^{0.5}}{2\pi\sigma_X}\right] \exp\left[\frac{-b^2}{2\sigma_X^2\left(1-\rho_{X\dot{X}}^2\right)}\right] + \left[\frac{\rho_{X\dot{X}}b\sigma_{\dot{X}}}{(2\pi)^{0.5}\sigma_X^2}\right] \exp\left(\frac{-b^2}{2\sigma_X^2}\right)\Phi\left[\frac{\rho b}{\sigma_X\left(1-\rho_{X\dot{X}}^2\right)^{\frac{1}{2}}}\right], \quad (27)$$

where $\sigma_X^2(t)$, $\sigma_{\dot{X}}^2(t)$, $\rho_{X\dot{X}}(t)$, and Φ are the variances of the process, its derivative, their correlation coefficient, and Gaussian (normal) CDF, respectively.

4.2. Vanmarcke approximation

Among the modification suggested for Poisson's method, the "Two-state process" assumption by Markov, or Vanmarcke [37] method has received more attention and is proper for narrow-band processes.

In this method, an envelope process is used to implement the independency of the "eligible" crossings. A crossing, with a positive slope, of level b by $X(t)$ envelope is called "eligible", only if it accompanies at least one positive passage of $|X(t)|$ from the same level. For a random, zero-mean, stationary Gaussian process of $X(t)$, Vanmarcke has proposed an approximate relation to be used instead of Eq. (26) [37]:

$$\eta_X^V(b,t) = 2\nu^+(b,t)\left\{\frac{1-\exp\left(-\left(\frac{\pi}{2}\right)^{0.5}q^{1.2}\left(\frac{b}{\sigma_X}\right)\right)}{1-\exp\left(-\frac{1}{2}\left(\frac{b}{\sigma_X}\right)^2\right)}\right\}. \quad (28)$$

This method calculates the stationary bandwidth factor based on the spectral moment of the process. For non-stationary processes, these values could be unbounded. Corotis et al. [38] have proposed an experimental method to calculate this value, which is only applicable to a certain case of the response of an SDOF system under a stationary excitation.

4.3. Michaelov-Lutes-Sarkani (MLS) method

Using Vanmarcke's approximation, Michaelov et al. [39] showed that for a more general non-stationary response, the crossing rate of the positive slope of the qualified envelope can be stated as below [40]:

$$\eta_X^V(x,t) = \frac{\left(1-F_V(x,t)\right)2\nu_X^+(0,t)}{F_V(x,t)}\cdot\left\{1-\exp\left[-\frac{V_V^+(x,t)}{\left[1-F_V(x,t)\right]2V_X^+(0,t)}\right]\right\}, \quad (29)$$

wherein, $F_V(x,t)$ and $V_V^+(x,t)$ are equal to the transient CDF and the unconditional rate of up-crossing of the envelope process $V(t)$. Considering the Probability Density Function (PDF) of the envelope process $p_V(x,t)$ and its joint distribution with $\dot{V}(t)$ for an evolutionary Gaussian process, it can be shown that Eq. (30) expresses the upcrossing rate of the qualified envelope [39] as shown in Box I, where $q_X(t)$ is the bandwidth factor and is derived in a way that it holds for a non-stationary process and $\Psi(x) = \exp\left(-x^2/2\right) + \sqrt{2\pi}\Phi(x)$. It can be observed that except for the experimental power of 1.2, for the case

$$\eta_X^V(x,t)=\frac{1}{\pi}\sqrt{1-\rho_{X\dot{X}}^2(t)}\frac{\sigma_{\dot{X}}(t)}{\sigma_X(t)}\times\frac{1-\exp\left[-\sqrt{\frac{\pi}{2}}\frac{x}{\sigma_x(t)}\sqrt{\frac{\left(q_X(t)^2-\rho_{X\dot{X}}^2(t)\right)}{1-\rho_{X\dot{X}}^2(t)}}\Psi\left(\frac{\rho_{X\dot{X}}(t)x}{\sqrt{q_X(t)^2-\rho_{X\dot{X}}^2(t)}\sigma_X(t)}\right)\right]}{\exp\left[\frac{x^2}{2\sigma_X^2(t)}\right]-1}. \quad (30)$$

Box I

in which $\rho_{X\dot{X}}(t)=0$, Eq. (28) and Eq. (30) yield identical results. This method hereafter will be denoted as "MLS".

5. Analytical response spectrum of DFM model in the frequency domain

If a linear elastic SDOF is subjected to a non-stationary excitation record, $a_{DFM}(t)$, derived from DFM, the response can be stated as:

$$\ddot{x}+2\xi_0\omega_0\dot{x}+\omega_0^2x=-a_{DFM}(t). \quad (31)$$

In this case, the response $x(t)$ can be rewritten in form of the convolution integral as below:

$$x(t)=-\int_0^t h_0(t-\tau)\,a_{DFM}(\tau)\,d\tau. \quad (32)$$

Substituting Eq. (11) in Eq. (32) gives:

$$x(t)=-\int_{-\infty}^{+\infty}\alpha(\tau_2)\int_{-\infty}^{+\infty}h_0(t-\tau_2)\,h(\tau_2-\tau_1,\tau_1)\,U(\tau_1)\,W(\tau_1)\,d\tau_1d\tau_2=-\int_{-\infty}^{+\infty}U(\tau_1)\,W(\tau_1)\int_{-\infty}^{+\infty}\alpha(\tau_2)\,h_0(t-\tau_2)\,h(\tau_2-\tau_1,\tau_1)\,d\tau_2d\tau_1. \quad (33)$$

Eq. (33) can be interpreted as the convolution of white noise and a combined IRF, $h_{x,comb}$, which can be stated as below:

$$h_{x,comb}(t-\tau_1,\tau_1)=U(\tau_1)\int_{-\infty}^{+\infty}\alpha(\tau_2)\,h_0(t-\tau_2)\,h(\tau_2-\tau_1,\tau_1)\,d\tau_2, \quad (34)$$

for $x(t)$ function, which is a non-stationary modulated process, the combined modulating function, $A_{x,comb}(t,\omega)$, can be stated as below:

$$A_{x,comb}(t,\omega)=\int_{-\infty}^{\infty}\exp\left[-i\omega(t-\tau_1)\right]U(\tau_1)\int_{-\infty}^{+\infty}\alpha(\tau_2)\,h_0(t-\tau_2)\,h(\tau_2-\tau_1,\tau_1)\,d\tau_2d\tau_1=\int_{-\infty}^{\infty}h_0(t-\tau_2)\,A(\tau_2,\omega)\exp\left[-i\omega(t-\tau_2)\right]d\tau_2\approx\overline{\tilde{A}(t,\omega)}H_0(\omega), \quad (35)$$

where $\overline{A(t,\omega)}$ is the mean value of $A(\tau,\omega)$ obtained from Eq. (19) for $0\le\tau\le t$.

A similar procedure can be done for $\dot{x}(t)$ to achieve $\tilde{A}_1(t,\omega)$ which is its modulating function.

$$\dot{x}(t)=-\int_0^t\dot{h}_0(t-\tau)\,a_{DFM}(\tau)\,d\tau. \quad (36)$$

Substituting Eq. (11) in Eq. (32) gives:

$$h_{\dot{x},comb}(t-\tau_1,\tau_1)=A(\tau_1)\int_{-\infty}^{+\infty}\alpha(\tau_2)\,\dot{h}_0(t-\tau_2)\,h(\tau_2-\tau_1,\tau_1)\,d\tau_2. \quad (37)$$

The modulating function for a non-stationary modulated process, $\dot{x}(t)$, can be stated as below:

$$A_{\dot{x},comb}(t,\omega)=\int_{-\infty}^{\infty}\exp\left[-i\omega(t-\tau_1)\right]U(\tau_1)\int_{-\infty}^{+\infty}\alpha(\tau_2)\,h_0(t-\tau_2)\,h(\tau_2-\tau_1,\tau_1)\,d\tau_2d\tau_1=\int_0^t h_0(t-\tau_2)\,A(\tau_2,\omega)\exp\left[-i\omega(t-\tau_2)\right]d\tau_2\approx\overline{A(t,\omega)}H_0(\omega)(i\omega). \quad (38)$$

To determine the peak factor with any method prescribed in Section 4, one could evaluate $\sigma_x(t)$, $\sigma_{\dot{x}}(t)$, $\rho_{x\dot{x}}(t)$, and $q(t)$ according to the following formulas [39]:

$$c_{00}(t)=2\int_0^\infty G_{XX}(t,\omega)\,d\omega=\sigma_x^2(t),$$

$$c_{11}(t)=2\int_0^\infty G_{\dot{X}\dot{X}}(t,\omega)\,d\omega=\sigma_{\dot{x}}^2(t),$$

$$c_{01}(t)=c_{01}^*(t)=-2i\int_0^\infty G_{x\dot{x}}(t,\omega)\,d\omega,$$

$$\rho_{X\dot{X}}(t)=-\frac{Im\left[c_{01}(t)\right]}{\sqrt{c_{00}(t)\,c_{11}(t)}},$$

$$q(t)=\sqrt{1-\frac{\left(Re\left[c_{01}(t)\right]\right)^2}{c_{00}(t)\,c_{11}(t)}}. \quad (39)$$

6. Time-domain equations for spectrum estimation

Computing $A_{x,comb}(t,\omega)$ and $A_{\dot{x},comb}(t,\omega)$ in the frequency domain is very hard and it seems that using the time-domain method is easier, therefore equations can be derived in the time domain. Having $h_{x,comb}(t,\tau)$ of

SDOF response from Eq. (34), the response variance can be stated as:

$$c_{00}(t) = E\left[\mathrm{X}^2(t)\right] = 2\pi \mathrm{S}_0 \int_{-\infty}^{+\infty} A^2(\tau) h_{\mathrm{x,comb}}^2(t,\tau)\, d\tau. \quad (40)$$

Similarly, for $\dot{x}(t)$, the variance can be calculated as:

$$c_{11}(t) = E\left[\dot{X}^2(t)\right] = 2\pi \mathrm{S}_0 \int_{-\infty}^{+\infty} A^2(\tau) h_{\dot{x},\mathrm{comb}}^2(t,\tau)\, d\tau, \quad (41)$$

and $E\left[X(t)\dot{X}(t)\right]$ can be expressed as:

$$-Im\left[c_{01}(t)\right] = E\left[X(t)\dot{X}(t)\right] = 2\pi \mathrm{S}_0 \int_{-\infty}^{+\infty} A^2(\tau) h_{\mathrm{comb}}(t,\tau) h_{\dot{x},\mathrm{comb}}(t,\tau)\, d\tau. \quad (42)$$

Now, $Y(t)$ which is the "auxiliary" process for evaluation of the bandwidth factor should be defined employing the following relation:

$$Y(t) = -\frac{1}{\pi}\int_{-\infty}^{+\infty}\int_{-\infty}^{\infty}\int_{-\infty}^{+\infty} A(\tau_1)\alpha(\tau_2) h_0(t-\tau_2) h(\tau_2-\tau_1,\tau_1)\frac{W(u)}{\tau_1-u} du d\tau_2 d\tau_1 = -\frac{1}{\pi}\int_{-\infty}^{+\infty} A(\tau) h_{\mathrm{x,comb}}(t,\tau)\int_{-\infty}^{\infty}\frac{W(u)}{\tau-u} du d\tau. \quad (43)$$

Now, to calculate $\dot{Y}(t)$ for the auxiliary process of displacement response, it can be also said that:

$$\dot{Y}(t) = -\frac{1}{\pi}\int_{-\infty}^{+\infty} A(\tau) h_{\dot{x},\mathrm{comb}}(t,\tau)\int_{-\infty}^{\infty}\frac{W(u)}{\tau-u} du d\tau, \quad (44)$$

based on which, $K_{X\dot{Y}}(t,t)$ can be calculated as:

$$\mathrm{Re}\left[\mathrm{c}_{01}(t)\right] = K_{X\dot{Y}}(t,t) = E\left[X(t)\dot{Y}(t)\right] = 2S_0 \int_{-\infty}^{+\infty}\int_{-\infty}^{\infty}\frac{h_{\mathrm{comb}}(t,\tau_1) h_{\dot{x},\mathrm{comb}}(t,\tau_2)}{\tau_2-\tau_1} A(\tau_1) A(\tau_2)\, d\tau_1 d\tau_2. \quad (45)$$

To calculate the above integration, a change of variable can be used to write:

$$\mathrm{Re}\left[\mathrm{c}_{01}(t)\right] = K_{X\dot{Y}}(t,t) = 2S_0 \int_0^t \frac{1}{u}\int_u^t h_{\mathrm{comb}}(t,\tau-u) h_{\dot{x},\mathrm{comb}}(t,\tau) A(\tau) A(\tau-u)\, d\tau du = 2S_0 \int_0^t \frac{1}{u}\int_u^t h_{\mathrm{comb}}(t,\tau-u) h_{\dot{x},\mathrm{comb}}(t,\tau)\, d\tau du. \quad (46)$$

Also, to calculate $q(t)$, $E\left[\dot{Y}^2(t)\right]$ should be calculated by the equations in previous sections which are equal to $\sigma_{\dot{X}}^2(t)$. In the next section, we compare the results from both time-domain and frequency-domain estimations for different approximations and Monte Carlo Simulation (MCS).

7. Results of the simulation

In this case, the results obtained from our semi-analytical methods have been compared with the 10000 MCSs. For this, Eq. (34) has been evaluated numerically at τ_2 with $n\Delta t$ with n equal to 100. The sensitivity analysis shows that this n value leads to fast simulations without compromising the accuracy of the estimation. Therefore the Eq. (35) can be expressed as the following expression:

$$A_{x,comb}(jn\Delta t,\omega) = n\Delta t \sum_{k=0}^{j-1} h_0(n\Delta t(j-k)) A(kn\Delta t,\omega)\exp\left[-i\omega n\Delta t(j-k)\right]. \quad (47)$$

Figure 2 compares the results of different methods for different values of the DFM model parameters. The plots indicate that difference between time-domain-based formulas and the frequency-domain-based formulations is not significant. It is observed that they have not been successful in estimating the peak of spectral acceleration at long periods. It is also seen that the frequency-domain calculations are more successful than time-domain calculations in predicting the response spectra for the very short-period region. Also, Figure 3 depicts the CDF of the maximum response of elastic SDOFs with different natural periods for the Vanmarcke formulation evaluated in the time domain. It is seen that the compatibility of the analytic MCS increases as the period rises.

To investigate the effect of inaccuracy in the estimation of $\sigma_X^2(t)$, $\sigma_{\dot{X}}^2(t)$, $\rho_{X\dot{X}}(t)$, and $q(t)$ on SD error, for some cases these values are estimated using the MCSs and they are inserted into Eq. (27), Eq. (28), and Eq. (30) to predict the median values of the peak response. Figure 4 shows the estimation error for a specific ensemble of DFM parameters. The results show that, compared to the case where these values are obtained from rigorous analytic function, even if the evolutionary features generated by simulation are used, it does not lead to the best approximation of the peak response factor. This indicates that the difference between the MLS and the proposed semi-analytic relationships does not stem from the inaccuracy of analytic estimation of $\sigma_X^2(t)$, $\sigma_{\dot{X}}^2(t)$, $\rho_{X\dot{X}}(t)$, and $q(t)$.

It should be mentioned that both MLS and Vanmarcke's methods need the bandwidth factor $q(t)$ for the peak factor to be evaluated. However, the

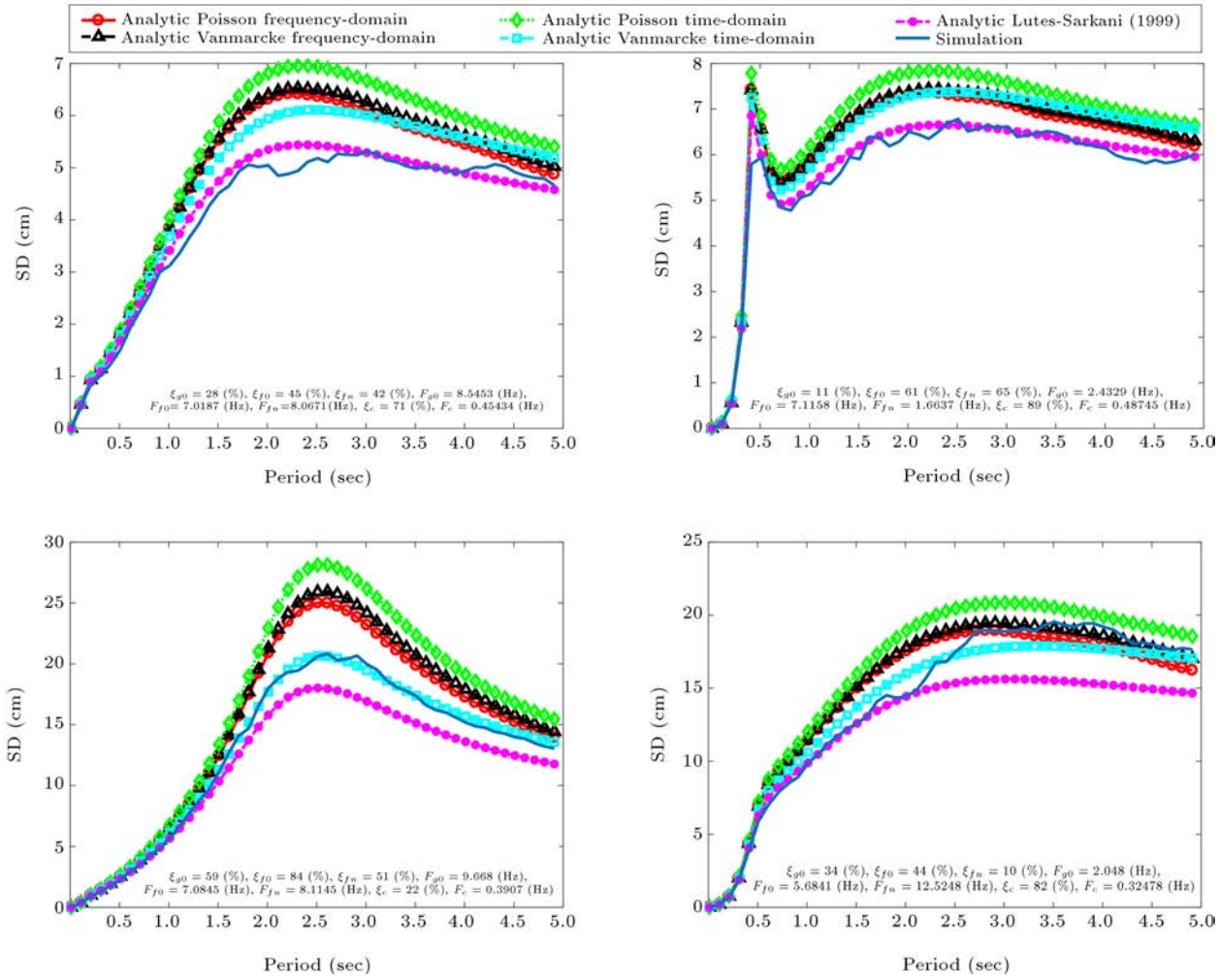

Figure 2. Comparison of different methods of median response spectrum approximation for records resulted from double-frequency method, using Poisson and Vanmarcke's approximations with frequency-domain methods adjusted.

effective evaluation of the $q(t)$ requires more complex computations needed for other parameters such as the variance of the displacement and velocity as well as their correlation coefficient. Moreover, it is very unlikely to get the bandwidth factor of a single output by applying the definition in Eq. (46). However, given the evolutionary characteristics of the process according to MCS the MLS formula yields the best results for the cases for which other methods show erroneous outputs. It can be deduced that the MLS is very sensitive to the evolutionary characteristics of the results and if it is fed with proper characteristics, it can be the most proficient method for evaluating the distribution of the peak values. This is not easy to achieve because it is not easy to predetermine the bandwidth $q(t)$ value using only model parameters.

It is seen that the results highly dependent on the correlation coefficient of the $\rho_{X\dot{X}}$ produce poor results. In most cases, the analytic expressions are unable to predict the maximum Pseudo-Acceleration Spectrum (SPA) value correctly. The results show that for methods involving correlation coefficient terms, even a few percentage points of error in the estimation of $\rho_{X\dot{X}}(t)$ would lead to drastic differences. Figure 5 shows the variation of SD estimation inaccuracy versus the difference of the analytical values of $\rho_{X\dot{X}}(t)$ from MCS and SDOF period using the Vanmarcke method. It is seen that for the MLS method, even a change of 0.04 in $\rho_{x\dot{x}}$ has increased the mean SD error by 15%. This proves the importance of using the MLS method, which more strictly incorporate $\rho_{x\dot{x}}$ into its relationship to determine the upcrossing rate.

It should be pointed out that the Monte Carlo-based estimation of parameters is not given in most of the cases and it is not easily calculated; therefore, the problem should be solved using analytic estimation of input parameters. Surprisingly, it is seen that there is a significant difference between the MLS method when input parameters of simulation or estimation are used. Hence, assuming that 3 of the 4 input parameters are given by analytic expressions, and one of them is adopted from the simulation method, the

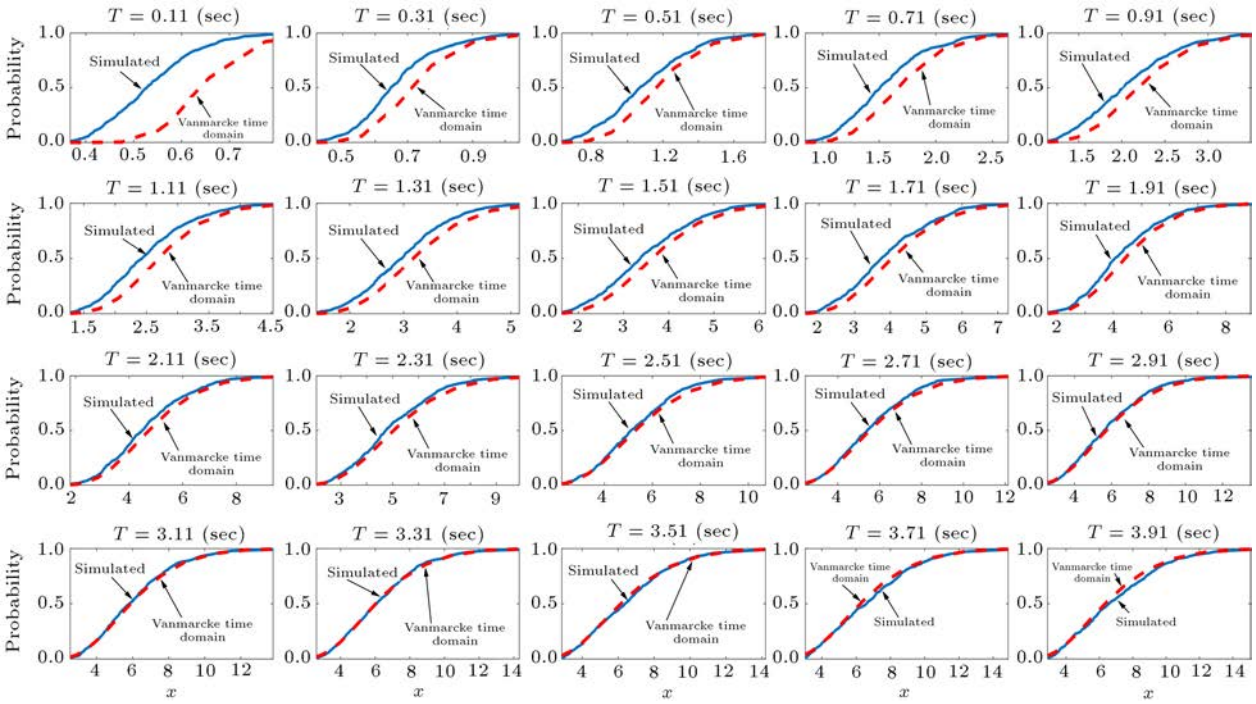

Figure 3. The cumulative distribution function of the maximum elastic response of Single Degrees-Of-Freedom (SDOF) with different natural periods subjected to Double-Frequency Model (DFM) excitation resulted from analytical method compared to Monte Carlo simulations.

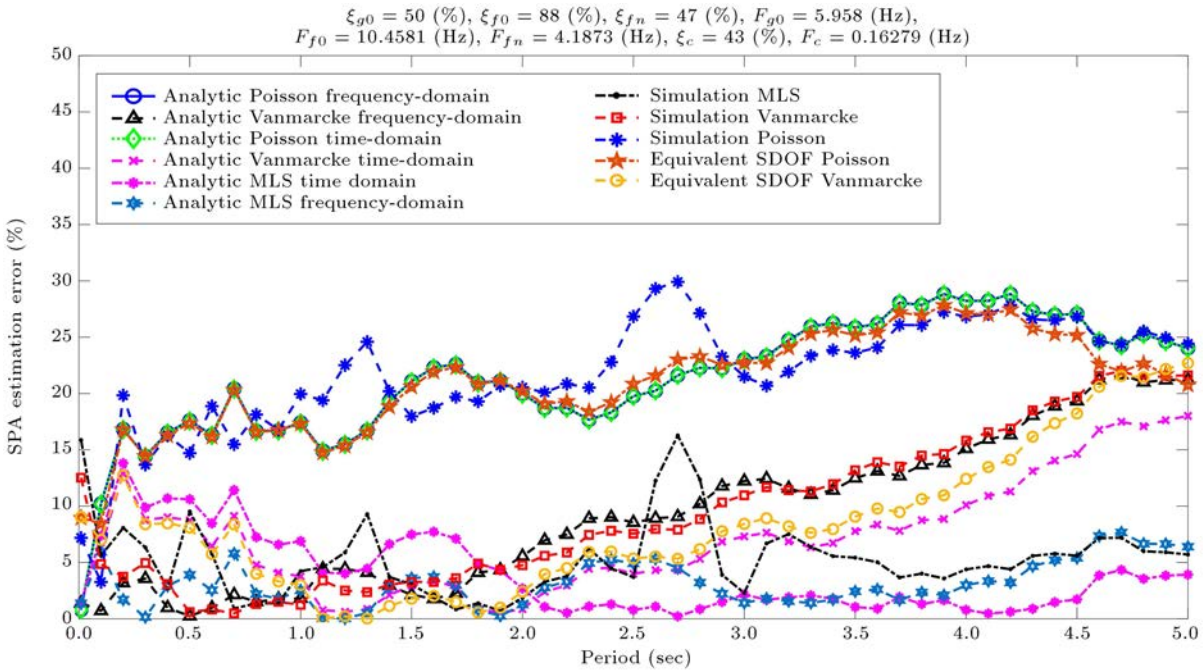

Figure 4. The efficiency of Michaelov-Lutes-Sarkani (MLS) method for estimation of the response spectrum given that evolutionary characteristics are calculated using Monte Carlo simulation.

analytic estimation of the spectral shift is repeated. Regarding the MLS method, it can be easily seen that when the simulation methods are used to calculate the correlation coefficient parameters, the results have been significantly improved. This shows that even a small amount of error in the estimation of the correlation coefficient will lead to disastrous results for MLS or any other method that is dependent on the correlation coefficient parameter. To circumvent this problem, two methods can be adopted: 1) to reduce the estimation

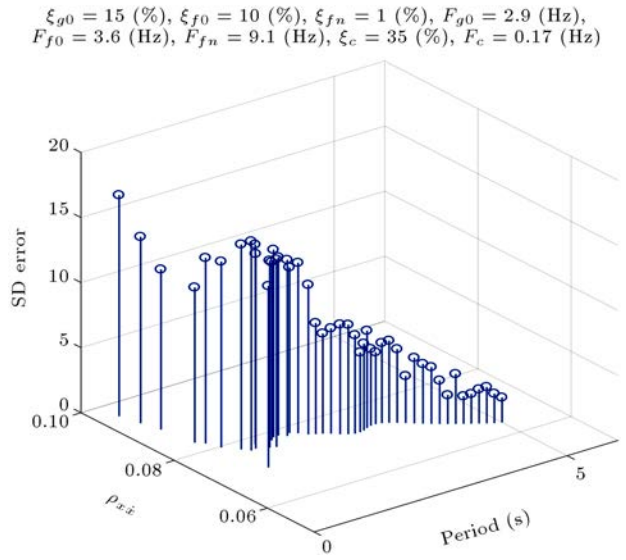

Figure 5. The variation of SD estimation inaccuracy vs. $\rho_{X\dot{X}}(t)$ and Single Degrees-Of-Freedom (SDOF) period for Vanmarcke's method.

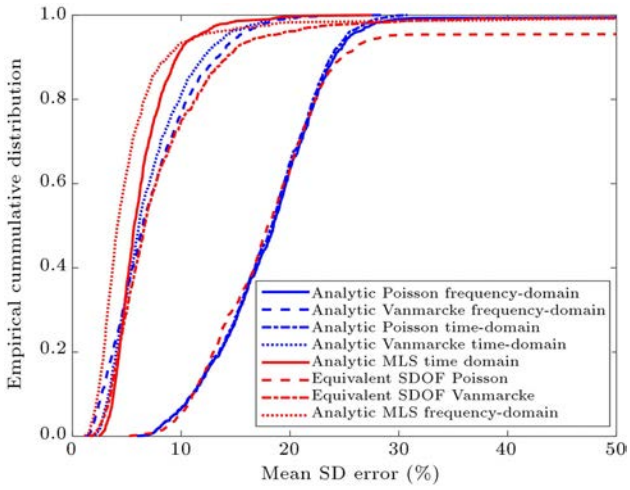

Figure 6. The empirical distribution function of the relative error of the analytical methods for estimating the response spectrum of the acceleration records generated from Double-Frequency Model (DFM).

error of the correlation coefficient by investigating the estimation error more; 2) to use the different methods for the short-term and long-term regions.

To evaluate the efficiency of each of the peak-factor methods, 10000 MCSs were completed. Thirteen model parameters were randomly generated to simulate artificial record accelerations, and then their response spectra are compared against the results obtained from analytical formulations. The empirical distribution function for the relative error of the median response spectrum and their analytical counterpart is shown in Figure 6. It is seen that the MLS method in the frequency-domain has exceeded every other method and yielded much better results. The results indicate

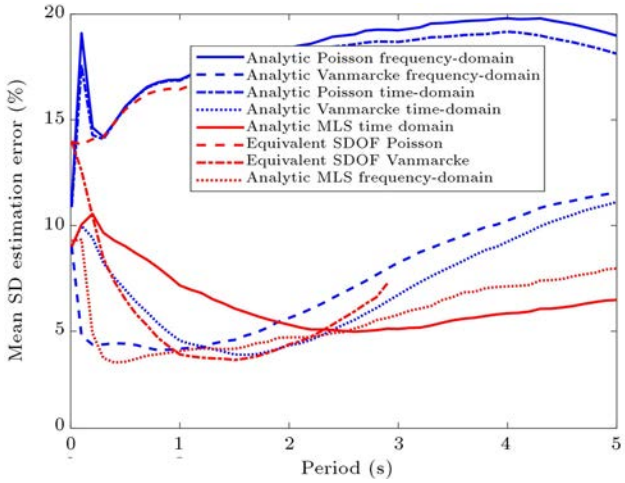

Figure 7. The variation of the mean relative error of SD estimated using analytic methods versus period of Single Degrees-0f-Freedom (SDOF) subjected to the acceleration records generated from Double-Frequency Model (DFM).

that this method can produce results with an error of less than 10% for 92% of the considered synthetic acceleration records. The semi-analytical method generates a mean SD error between 10% and 40% for the other 8% of the records. However, MLS's method using the time-domain formulation has the same number of cases as those of the frequency-domain method with a mean SD error less than 10% . On the other hand, the frequency-domain formulation has provided fewer cases with a mean SD error between 10% and 20%. The time-domain method yields SD estimations with the maximum mean error as much as 20% while the frequency-domain case may even lead to mean SD results as large as 40%.

Figure 7 illustrates the dependence of SD estimation error on the natural period of SDOF on which DFM record is applied. It is found that when the period becomes higher than 1 s, the accuracy of all of the methods decreases. Also, when the period drops, the frequency-based formulation produces better results. It is seen that for most of the period ranges MLS is the most efficient method for estimating the results of the spectrum compared to Poisson and Vanmarcke methods. Given that the evolutionary properties of the time histories are generated according to frequency-domain results, MLS produces the best estimations for periods lower than 2 s. On the contrary, for the long-period region, there is a good agreement between the results of MCS and those obtained from the MLS method wherein the evolutionary characteristics obtained from time-domain analytic expressions are used.

It is also worth noting that Vanmarcke methods deviate rapidly ($> 5\%$ estimation error) for periods higher than 1–1.5 s. By employing the MLS method better results could be obtained, therefore it can be

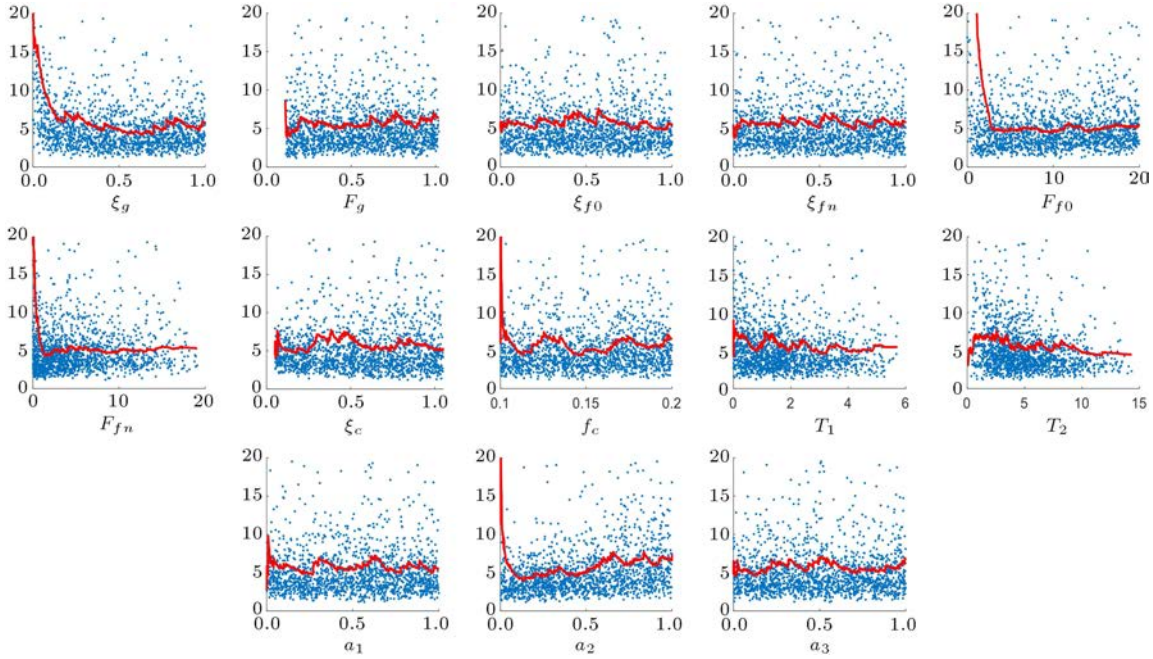

Figure 8. Correlation between the mean SD errors estimated from Michaelov-Lutes-Sarkani MLS frequency-domain formulation and the Double-Frequency Model (DFM) parameters (red lines depict the moving average with a window size of 100).

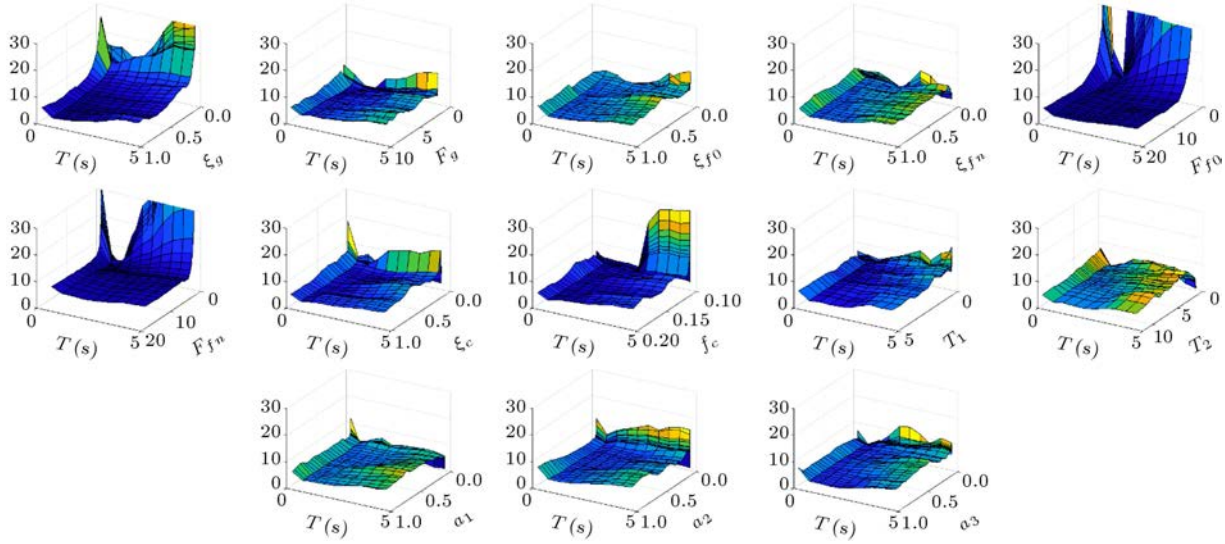

Figure 9. Correlation between the mean SD errors for a different period ranges estimated from Michaelov-Lutes-Sarkani (MLS) frequency-domain formulation and the Double-Frequency Model (DFM) parameters.

deduced that assuming zero correlation coefficient for long-period SDOF response to DFM excitation leads to a drastic error. This outcome can be further investigated by comparing the poor results of the Poisson method with other methods for all period ranges. This is due to the fact that in the estimation of crossing level by the Poisson method, compared to Vanmarcke and MLS, the bandwidth factor is not considered. This shows the importance of considering the bandwidth factor in the accuracy of semi-analytic estimation.

Figure 8 demonstrates the correlation between the mean SD errors estimated from MLS's frequency-domain formulation and the DFM parameters. It is seen that as ξ_g, f_{f0} or f_{f_n} decrease, the results of SD estimation get inferior. Also, the semi-analytic estimations generate slightly more erroneous results as f_c or a_2 decrease. There is no discernable relationship between mean error and other DFM parameters.

The same procedure is repeated for the mean SD error for different period ranges and the results are depicted in Figure 9. It is seen that as ξ_g, f_{f0} and f_{f_n} decrease, the error in estimating the spectral

response of longer periods increases significantly. It is also seen that as f_c decreases, the mean SD error for longer periods (> 2.5 s) rises whereas the change of the general trend of the SD error with DFM parameters is not considerable. Also, it is seen that as ξ_g or ξ_f decrease to values lower than 10%, the semi-analytic procedure for the period values corresponding to their frequency counterpart, i.e. f_g and f_{f0}, yields inferior estimations.

8. Conclusion

This paper presents a semi-analytical method for estimating the elastic response spectra of acceleration records generated by the site-based Double-Frequency Model (DFM) method. Therefore, different estimation procedures based on Vanmarck, Poisson, and Michaelov assumptions are implemented to solve the "first passage problem". For this reason, the variance of the displacement and velocity responses of an elastic Single Degrees-Of-Freedom (SDOF) as well as their correlation coefficient and bandwidth factor subjected to the DFM acceleration records have been determined analytically in time and frequency domains. It is assumed that the envelope function of the DFM is a slowly varying function of time. Also, the evolutionary transfer function of the system is considered to be varying slow enough that the instantaneous Evolutionary Power Speetral Density (EPSD) can be estimated according to the temporal average of the modulating function of the response process. The foretold statistical parameters required for analytical methods are numerically determined according to the definition of the DFM method and their accuracy is evaluated via Monto Carlo Simulation (MCS). Thereafter, the median values of the displacement maximum response are evaluated for 10000 realizations of the DFM acceleration records to determine their elastic response spectrum. The estimation procedure is implemented in the time and frequency domains. The results show that by using the MLS assumption in the frequency domain it will be possible to predict 92% of the response spectrum of the considered synthetic acceleration records with an error of less than 10%. The semi-analytical method generates a mean SD error between 10% and 40% for the other 8% of the records. In addition, compared to other procedures, the MLS formula executed in the frequency domain produces the best results. This shows that it is necessary to incorporate the process correlation coefficients, their derivatives, and their bandwidths into the analytical estimation procedure. However, the time-domain estimations result to less compatible response spectra at lower periods. Based on the slow-varying assumptions on the modulating function, as the time-varying parameters of the DFM model, i.e. $f_f(t)$ and $\xi_f(t)$, change faster with time, the efficiency of the model will be decreased. Also, it is seen that when the damping values corresponding to the peak frequencies of the model decrease to values lower than 10%, the semi-analytic procedure for the period values corresponding to their frequency counterpart yields inferior estimations.

References

1. Rezaeian, S. and Der Kiureghian, A. "A stochastic ground motion model with separable temporal and spectral nonstationarities", *Earthquake Eng. Struct. Dyn.*, **37**(13), pp. 1565–1584 (2008).
2. Stafford, P., Sgobba, S., and Marano, G. "An energy-based envelope function for the stochastic simulation of earthquake accelerograms", *Soil Dyn. Earthquake Eng.*, **29**, pp. 1123–1133 (2009).
3. Maechling, P.J., Silva, F., Callaghan, S., and Jordan, T.H. "SCEC Broadband Platform: System architecture and software implementation", *Seismol. Res. Lett.*, **86**(1), pp. 27–38 (2014).
4. Sun, X., Hartzell, S., and Rezaeian, S. "Ground-motion simulation for the 23 august 2011, mineral, virginia, earthquake using physics-based and stochastic broadband methods", *Bull. Seismol. Soc. Am.*, **105**(5), pp. 2641–2661 (2015).
5. Kramer, S.L., *Geotechnical Earthquake Engineering*, **80**, Prentice Hall Upper Saddle River, NJ (1996).
6. Li, Y., Conte, J.P., and Barbato, M. "Influence of time-varying frequency content in earthquake ground motions on seismic response of linear elastic systems", *Earthquake Eng. Struct. Dyn.*, **45**(8), pp. 1271–1291 (2016).
7. Kiureghian, A.D. and Crempien, J. "An evolutionary model for earthquake ground motion", *Struct. Saf.*, **6**, pp. 235–246 (1989).
8. Beresnev, I. and Atkinson, G. "FINSIM: A FORTRAN program for simulating stochastic acceleration", *Seismol. Res. Lett.*, **69**, pp. 27–32 (1998).
9. Motazedian, D. and Atkinson, G. "Stochastic finite-fault modeling based on a dynamic corner frequency", *Bull. Seismol. Soc. Am.*, **95**(3), pp. 995–1010 (2005).
10. Papadimitriou, K. "Stochastic characterization of strong ground motion and application to structural response", *Pasadena*, CA EERL 90-03 (1990).
11. Pousse, G., Bonilla, L., Cotton, F., and Margerin, L. "Non stationary stochastic simulation of strong ground motion time histories including natural variability: Application to the K-net Japanese database", *Bull. Seismol. Soc. Am.*, **96**(6), pp. 2103–2117 (2006).
12. Yamamoto, Y. and Baker, J.W. "Stochastic model for earthquake ground motion using wavelet packets", *Bull. Seismol. Soc. Am.*, **103**(6), pp. 3044–3056 (2013).
13. Shinozuka, M. and Deodatis, G. "Stochastic process models for earthquake ground motion", *Probabilist. Eng. Mech.*, **3**(3), pp. 114–123 (1988).

14. Chen, J., Kong, F., and Peng, Y. "A stochastic harmonic function representation for non-stationary stochastic processes", *Mech. Syst. Signal. Pr.*, **96**, pp. 31–44 (2017).

15. Rezaeian, S. and Der Kiureghian, A. "Simulation of synthetic ground motions for specified earthquake and site characteristics", *Earthquake Engineering & Structural Dynamics*, **39**(10), pp. 1155–1180 (2010).

16. Waezi, Z. and Rofooei, F.R. "On the evolutionary characteristics of the acceleration records generated from linear time-variant systems ", *Sci. Iranica*, **26**(6), pp. 2817–2831 (2017).

17. Waezi, Z. and Rofooei, F.R. "Stochastic non-stationary model for ground motion simulation based on higher-order crossing of linear time variant systems", *J. Earthquake Eng.*, **21**(1), pp. 1–28 (2016).

18. Waezi, Z., Rofooei, F.R., and Hashemi, M.J. "A multi-peak evolutionary model for stochastic simulation of ground motions based on time-domain features", *J. Earthquake Eng.*, **25**(2), pp. 1–37 (2018).

19. Alderucci, T., Muscolino, G., and Urso, S. "Stochastic analysis of linear structural systems under spectrum and site intensity compatible fully non-stationary artificial accelerograms", *Soil Dyn. Earthquake Eng.*, **126**, p. 105762 (2019).

20. Kiureghian, A.D. and Fujimura, K. "Nonlinear stochastic dynamic analysis for performance-based earthquake engineering", *Earthquake Eng. Struct. Dyn.*, **38**(5), pp. 719–738 (2009).

21. Ferrer, I. and Sánchez-Carratalá, C.R. "Efficient estimation of the peak factor for the stochastic characterization of structural response to non-stationary ground motions", *Struct. Saf.*, **59**, pp. 32–41 (2016).

22. Michaelov, G., Lutes, L.D., and Sarkani, S. "Extreme value of response to nonstationary excitation", *J. Eng. Mech.*, **127**(4), pp. 352–363 (2001).

23. Barbato, M. and Vasta, M. "Closed-form solutions for the time-variant spectral characteristics of non-stationary random processes", *Probabilist. Eng. Mech.*, **25**(1), pp. 9–17 (2010).

24. Barbato, M. and Conte, J.P. "Structural reliability applications of nonstationary spectral characteristics", *J. Eng. Mech.*, **137**(5), pp. 371–382 (2011).

25. Clough, R.W. and Penzien, J., *Dynamics of Structures*, 2nd Ed., Berkeley, CA USA: Computers & Structures, Inc. (1993).

26. Barbato, M. and Conte, J.P. "Time-variant reliability analysis of linear elastic systems subjected to fully nonstationary stochastic excitations", *J. Eng. Mech.*, **141**(6), p. 04014173 (2015).

27. Alderucci, T. and Muscolino, G. "Time-frequency varying response functions of non-classically damped linear structures under fully non-stationary stochastic excitations", *Probabilist. Eng. Mech.*, **54**, pp. 95–109 (2018).

28. Yu, H., Wang, B., Gao, Z., and Li, Y. "An exact and efficient time-domain method for random vibration analysis of linear structures subjected to uniformly modulated or fully non-stationary excitations", *J. Sound Vibrat.*, **488**, p. 115648 (2020).

29. Zhao, N. and Huang, G. "Efficient nonstationary stochastic response analysis for linear and nonlinear structures by FFT", *J. Eng. Mech.*, **145**(5), p. 04019023 (2019).

30. Xu, J. and Feng, D.-C. "Stochastic dynamic response analysis and reliability assessment of non-linear structures under fully non-stationary ground motions", *Struct. Saf.*, **79**, pp. 94–106 (2019).

31. Xu, J., Ding, Z., and Wang, J. "Extreme value distribution and small failure probabilities estimation of structures subjected to non-stationary stochastic seismic excitations", *Struct. Saf.*, **70**, pp. 93–103 (2018).

32. Waezi, Z. and Rofooei, F.R. "Stochastic non-stationary model for ground motion simulation based on higher-order crossing of linear time variant systems", *J. Earthquake Eng.*, **21**(1), pp. 123–150 (2017).

33. Amin, M. and Ang, A.H. "Nonstationary stochastic models of earthquake motions", *J. Eng. Mech.*, **94**(2), pp. 559–584 (1968).

34. Priestley, M.B. "Evolutionary spectra and non-stationary processes", *J. Roy. Stat. Soc. Ser. B. (Stat. Method.)*, **27**(2), pp. 204–237 (1965).

35. Senthilnathan, A. and Lutes, L.D. "Nonstationary maximum response statistics for linear structures", *J. Eng. Mech.*, **117**(2), pp. 294–311 (1991).

36. Shinozuka, M. and Yang, J.-N. "Peak structural response to non-stationary random excitations", *J. Sound Vibrat.*, **16**(4), pp. 505–517 (1971).

37. Vanmarcke, E.H. "On the distribution of the first-passage time for normal stationary random processes", *Journal of Applied Mechanics*, **42**(1), pp. 215–220 (1975).

38. Corotis, R.B., Vanmarcke, E.H., and Cornell, A.C. "First passage of nonstationary random processes", *J. Eng. Mech.*, **98**(2), pp. 401–414 (1972).

39. Michaelov, G., Sarkani, S., and Lutes, L. "Spectral characteristics of nonstationary random processes-response of a simple oscillator", *Struct. Saf.*, **21**(3), pp. 245–267 (1999).

40. Lutes, L.D. and Sarkani, S., *Random Vibrations: Analysis of Structural and Mechanical Systems*, Burlington, MA 01803, USA: Butterworth-Heinemann (2004).

Biographies

Zakariya Waezi has been an Assistant Professor of Civil Engineering at Shahed University, Iran, since 2016. He received his BSc degree in Civil and Petroleum Engineering his MSc degrees in Earthquake Engineering and also his PhD degree in the

Structural/Earthquake Engineering from the Sharif University of Technology. His research interests are random vibrations, nonlinear structural analysis, and assessment of the seismic performance of structures.

Mohammad Amin Raoof is a graduate student of Civil Engineering at the Sharif University of Technology, Tehran, Iran. He received his BSc degree in Civil Engineering from the Shahed University in 2018 and his MSc degree in Environmental Engineering from the Sharif University of Technology in 2020. His current research relates to predicting and simulating socio-technical drivers of consumer behavior in the field of urban water consumption. His research interests are complex socio-economic systems, coupled human-nature systems, agent-based modeling, remote sensing, behavior identification and prediction, decision-making, and machine learning.